Quasi-Phase Matching Magneto-Optical Waveguides

David C. Hutchings and Barry M. Holmes
School of Engineering, University of Glasgow, Glasgow G12 8QQ, U.K.

ABSTRACT

Photonic integration has proved remarkably successful in combining multiple optical devices onto a single chip with the benefits of added functionality, and reduction in costs, arising from the replacement of manual assembly and alignment of individual components with lithographic techniques. However, the incorporation of optical isolators and related non-reciprocal devices within standard optoelectronic wafer platforms is exceptionally challenging. Preferred magneto-optic materials cannot be exploited as waveguide core layers on semiconductor wafers due to a lower refractive index. Another difficulty is the phase velocity mismatch as a consequence of the inherent structural birefringence associated with waveguide geometries.

Our approach to the integration of an optical isolator with a III-V semiconductor laser involves combining a nonreciprocal mode converter with a reciprocal mode converter, based on an asymmetric profiled rib waveguide, fabricated by Reactive Ion Etching. We demonstrate that suitably tapered waveguides can be employed to connect the mode converter to other sections thereby avoiding problems caused by mode-matching and reflections from the section interfaces.

The nonreciprocal mode converter is formed from a continuation of the III-V semiconductor waveguide core with a magneto-optic upper cladding so that Faraday rotation occurs through the interaction of the evanescent tail. The phase velocity mismatch due to the waveguide birefringence is overcome using a quasi-phase-matching approach. Lithography is used to pattern the top cladding so that the film immediately on top of the waveguide core alternates between magneto-optic and a non-magneto-optic dielectric of a similar refractive index. Our first demonstrations used a dielectric (silica or silicon nitride) patterned by etching, or lift-off, on top of a GaAs rib waveguide, over which was deposited a magneto-optic film. This film was deposited by sputtering from a Ce:YIG target and demonstrated magnetic hysteresis, but, as it was not annealed, it was believed to consist of Ce:YIG and/or gamma iron oxide microcrystallites embedded in an amorphous matrix. With quasi-phase-matching periods of 110–160 μm and a waveguide length of 8 mm, we were able to demonstrate up to 12% non-reciprocal TE- to TM-mode conversion around a wavelength of 1.3 μm using the remanent magnetisation.

In order to enhance the magneto-optic effect it is desirable to anneal such films. However the mismatch in thermal expansion coefficients results in a catastrophic failure of samples with large area film coverage. This problem has been shown to be alleviated by patterning the YIG film. Unfortunately wet-etching of YIG also etches (Al)GaAs and, therefore, the development of a lift-off process for YIG deposition has been undertaken. Initial results are promising with $\sim$100 μm$\times$2.5 μm YIG sections deposited on a GaAs layer which remain intact after an anneal in an oxygen atmosphere.

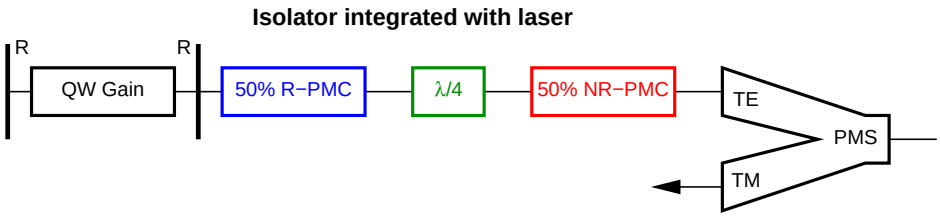

Figure 1: Block diagram of an optical isolator, comprising reciprocal and nonreciprocal polarisation mode converters, integrated with a semiconductor laser. A polarisation mode splitter (PMS) is additionally added to the device to ensure that only TE-polarised light is returned to the isolator. The PMS can be omitted should the downstream system preserve the polarisation state.

INTRODUCTION

Nonreciprocal optical elements are essential components in a range of optical systems. Optical isolators are used to protect optical sources, such as distributed feedback lasers in communication systems, which can have their stability comprimised by the injection noise resulting from unintended back-reflections in the system. Optical circulators are used to route optical signals to alternate ports depending on the direction of propagation, and are routinely deployed in optical fibre systems where reflective optical elements are exploited, such as bragg gratings for filtering or optical interfacial sensing elements. Current implementations of nonreciprocal optical devices use bulk components and are generally based upon Faraday rotation. These require assembly from individual constituents, with the associated additional costs and yield implications, and require the complexities of alignment to the external system, which may be guided-wave such as optical fibre.

The prospect of monolithically integrated nonreciprocal polarisation components, where lithography is used to define the components, has attracted considerable interest. There are two principal approaches: (1) the transverse magneto-optic effect can be used with metallic ferromagnetic layers in a semiconductor optical amplifier to obtain a nonreciprocal optical loss [1, 2]; (2) the longitudinal magneto-optic effect can be used, as in the bulk, to provide Faraday rotation and hence conversion between orthogonal polarisation modes. Here we provide innovative waveguide solutions to the latter.

There are a number of inherent difficulties in transferring the functionality of the components of a bulk isolator to an integrated format. First, while it is possible to devise polarisation selectivity for TE- or TM-polarised modes, it is not straightforward to replicate this selectivity for an arbitrarily orientated polariser, in particular at 45°. Our solution is to additionally incorporate a reciprocal polarisation mode converter (R-PMC) section, which provides the functionality of an appropriately orientated half-wave-plate [3], as shown in fig. 1. Second, YIG and related garnets are overwhelmingly suited to magneto-optic effects in propagation with a large Verdet constant and low optical loss, but have refractive indices substantially lower than the III-V semiconductor materials used in laser diodes. In order to effectively guide light, the refractive index of the core layer must normally be greater than that of the cladding layers. This, therefore, normally precludes the incorporation of conventional MO materials as waveguide core layers in III-V structures. However, this dichotomy may be circumvented through the integration of the MO media as an upper cladding layer [3, 4].

A further difficulty arises as a consequence of the inherent structural birefringence usually associated with planar waveguide formats. Nonreciprocal mode conversion through Faraday rotation

occurs because of an induced difference in the propagation constants for circularly polarised light $\Delta\beta_{\mathrm{MO}}$. However, with a structural birefringence $\Delta\beta_{\mathrm{S}}$ typically much larger, $\Delta\beta_{\mathrm{S}} \gg \Delta\beta_{\mathrm{MO}}$, the polarisation state undergoes an oscillatory behaviour with a limited maximum change occuring after propagating a specific distance denoted as the half-beat-length or coherence length,

$$L_c = \frac{\pi}{\sqrt{(\Delta\beta_{\mathrm{S}})^2 + (\Delta\beta_{\mathrm{MO}})^2}} \approx \frac{\pi}{|\Delta\beta_{\mathrm{S}}|} \quad .$$

After this distance, the phase relationship between modes has evolved such that the direction of the power flow between modes reverses and the polarisation state begins to revert to the original state. In semiconductor rib waveguides the coherence length is typically of the order of 100 μm or shorter.

Quasi-phase-matching (QPM) is a technique developed initially for nonlinear frequency conversion where the medium is structured periodically (with a period set to an odd integer of twice the coherence length) to compensate for a similar phase velocity mis-match between frequency components. QPM can be extended to magneto-optic waveguides and earlier attempts include a periodic current reversal [5] and localised annealing of a magneto-optic waveguide core [6]. Here we use an upper cladding that periodically alternates between magneto-optic and non-magneto-optic media and thus only requires the application of a unidirectional longnitudinal magnetic field.

THEORY

A coupled-mode analysis provides a useful and simple method for obtaining the evolution of the polarisation state through a waveguide device consisting of cascaded sections. It will be assumed that each section supports just two orthogonally polarised guided modes Ψ_{n1} and Ψ_{n2}, and therefore guided light after propagating a particular distance z in the device is a linear combination of these $a(z)\Psi_{n1} + b(z)\Psi_{n2}$, where $a(z)$ and $b(z)$ are, in general, complex. We assume, that for a coupled-mode analysis to be valid, optical losses through absorption, scattering to radiation modes or back-reflections at the transition between sections can be neglected. This may require a graded or tapered-feature transition, as has been demonstrated for the asymmetric rib waveguides fabricated using a Reactive Ion Etching (RIE) lag process [7]. The evolution of the guided light can be obtained using a transfer matrix approach with complex 2×2 matrices used to account for propagation within a section or the transition from one section to another.

We make two further modifications to this analysis. The initial and final waveguides section in such a device would usually be symmetric, non-magneto-optic wavguides. The fundamental modes of such a waveguide are conventionally termed “transverse-electric” (TE), where the light is predominantly polarised in the plane of the wafer, or “transverse-magnetic” (TM) where the light is predominantly polarised normal to the plane of the wafer. Note that for rib waveguides there is normally some degree of hybridisation for both of these modes so such descriptors are not strictly accurate. We will use the modes of such a waveguide as the basis set such that the polarisation state at distance along the waveguide device is characterised by the combination of TE- and TM-modes, $a(z)\Psi_{\mathrm{TE}} + b(z)\Psi_{\mathrm{TM}}$, that would be launched if a transition to the basis symmetric, non-magneto-optic wavguide occured at this position. For visualisation purposes, we now substitute the complex

a, b with 3 real, normalised effective Stokes parameters,

$$S_1 = (aa^* - bb^*)/(aa^* + bb^*)$$
$$S_2 = (ab^* + a^*b)/(aa^* + bb^*)$$
$$S_3 = -\mathrm{i}(ab^* - a^*b)/(aa^* + bb^*)$$

The locus of the Stokes vector $\mathbf{S} = (S_1, S_2, S_3)$ is on a unit radius sphere: the modified Poincaré sphere. The evolution of the polarisation state on propagation can be traced as a continuous trajectory on the surface of the modified Poincaré sphere. Within each waveguide section the trajectory is obtained by a rotation about an axis that intersects the Stokes vectors corresponding to the fundamental modes within that section. For a symmetric, non-magneto-optic wavguide this rotation axis is the S_1 axis. The incorporation of a longitudinal magneto-optic effect offsets this rotation axis towards the S_3 axis such that it is aligned along $(\Delta\beta_{\mathrm{S}}, 0, \Delta\beta_{\mathrm{MO}})$. For a non-magneto-optic, asymmetric profile waveguide the rotation axis lies within the $S_3 = 0$ plane.

One possible solution to the reciprocal polarisation mode converter requirements is a quarter beat length of an asymmetric waveguide with modes corresponding to $|a| = |b|$, i.e. a rotation axis corresponding to the S_2 axis. However this waveguide solution can only be approached asymptotically with increasingly tight tolerance requirements. Instead we propose to use a half-beat-length of an asymmetric waveguide with a rotation axis that lies at 45° to the S_1 and S_2 axes. The required mode transformation can be optimised by bracketing the required solution, and the tolerances for such a structure are relaxed. In terms of the RIE-lag method, a single trench design would suffice. The isolator design in this case would additionally incorporate a quarter-beat-length of a symmetric waveguide as illustrated in fig. 1.

The trajectories on the modified Poincaré sphere are shown in fig. 2 for the schematic integrated isolator device given in fig. 1. The left trajectory shows the TE-polarised emission from the laser $\mathbf{S} = (1, 0, 0)$ undergo a transformation (blue) to a 50:50 TE:TM polarised state in the reciprocal polarisation mode converter followed by a quarter-beat-length of a symmetric waveguide (green). There then follows the quasi-phase-matched section consisting of a sequence of coherence length sections periodically alternating between magneto-optic (red) and non-magneto-optic (green) until the polarisation state is returned to a TE-polarised state $\mathbf{S} = (1, 0, 0)$. The right trajectory shows the evolution of a TE-polarised input which first enters the QPM section. Note that the reversal of the direction of propagation reverses the relative direction of the magnetic field to the propagation, and consequently the sign of $\Delta\beta_{\mathrm{MO}}$) so the rotation axis is offset in the opposite direction. Similarly, the asymmetric profile of the reciprocal polarisation mode converter is the mirror image with respect to the direction of propagation and the appropriate axis of rotation is also the mirror image. It can be seen that following the final reciprocal polarisation mode converter the output is TM-polarised $\mathbf{S} = (-1, 0, 0)$. A normal quantum well laser, with the absence of the heavy-hole resonance for TM-polarised light, provides the final polarisation selectivity.

EXPERIMENT

Preliminary devices for a proof-of-principle study of QPM nonreciprocal mode conversion were fabricated [8]. These consisted of a 2.7 μm wide and 500 nm thick GaAs waveguide core on top of a $Al_{0.27}Ga_{0.73}As$ lower cladding formed by reactive ion etching to a depth of $\sim$600 nm. Periodic

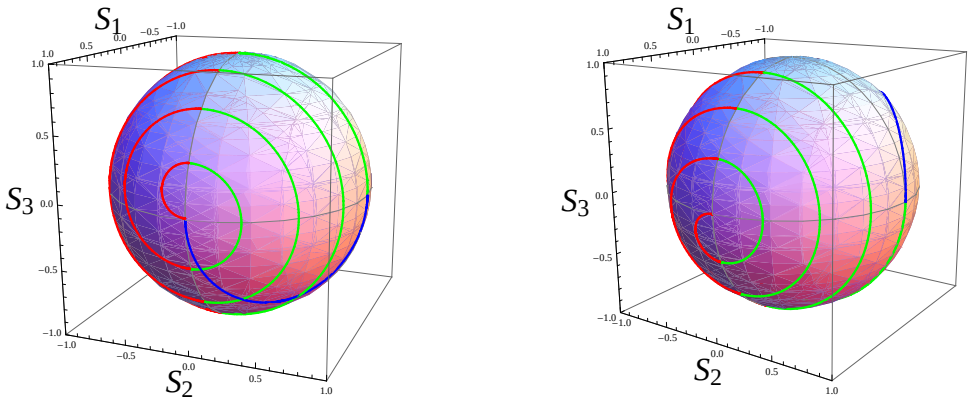

Figure 2: Polarisation state evolution shown as trajectories from a launched TE-polarised mode on the modified Poincaré sphere for forward (left) and backward (right) propagating light in the integrated optical isolator.

sections of a dielectric film were fabricated on top of this waveguide. Initially this was achieved by wet-etching the ∼200 nm thick SiO_2 hard mask used in the waveguide fabrication. In a later generation of samples, the dielectric sections were formed using a lift-off process with a Si_3N_4 film which showed an improvemed definition in the lithographic pattern transfer. The sample, with a substrate temperature of 60°C, was then sputter coated using a CeYFeO target (achieving $Ce_1Y_2Fe_5O_x$ stochiometry measured through the use of energy dispersive x-ray techniques). The ferromagnetic properties of this MO layer were obtained using the longitudinal Kerr effect, yielding a coercivity of 3.2 kAm^{-1} and a squareness of 0.7.

The periodicity of the alternating MO/non-MO upper cladding layer can be clearly observed in the SEM of a completed sample displayed in fig. 3 (left). The raised sections incorporate a ∼200 nm thick dielectric "exclusion" layer between the GaAs core and the CeYFeO upper cladding, effectively eliminating any interaction between the evanescent tail of the guided mode and the MO layer. In contrast, the non-raised sections consist of CeYFeO deposited directly upon the waveguide core, facilitating interaction with the guided modes.

The SiO_2 exclusion layer samples were saturated in a 240 kAm^{-1} magnetic field, applied parallel to the waveguides. The 8 mm long waveguides (equivalent to ∼60 periods) were then characterized without an external applied magnetic field, over a range of wavelengths using a tunable diode laser. Transverse electric (TE) polarised radiation was coupled into the guides using the end-fire technique and the output passed through a polarising beam-splitting cube in order to separate the TE- and TM-components. These were then individually detected to obtain the mode conversion efficiencies.

Fig. 3 (right) shows the dependence of the TM-polarised purity (ratio of the output power passed by a TM-polariser to the total output power) for a TE-polarised input as a function of wavelength for the three QPM periods 110, 120 and 130 μm. The lines are weighted least-square fits to a $sinc^2$ curve typical of phase-matched conversion processes and indicate an approximate linear dependence of the phase-matching wavelength on the grating period. Nonreciprocal behaviour was verified by analysing the relative phase of the TE- and TM-polarised components which are observed to reverse upon turning the sample around, or by reversing the direction of the magnetising field. Optical losses in the waveguides were observed to be around 1 dB/mm. In this investiga-

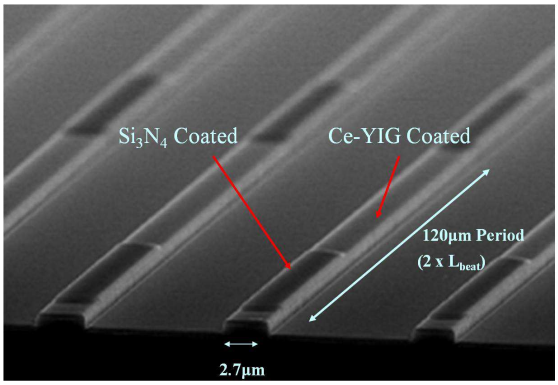

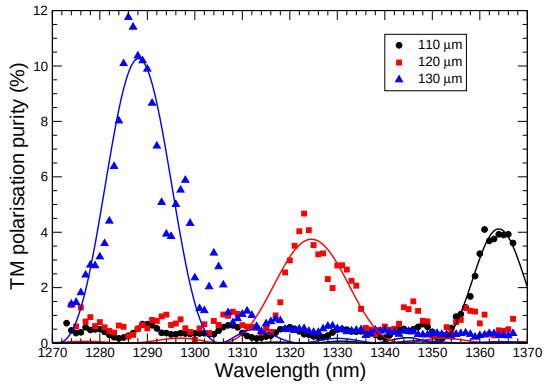

Figure 3: Fabricated QPM nonreciprocal mode conversion rib waveguides with a GaAs core and SiO_2/CeYFeO upper cladding (left). Measured TM-polarised purity for a TE-polarised input as a function of wavelength for the three QPM periods shown (right).

tion the largest observed TE- to TM-polarisation conversion is 12%, obtained at a wavelength of 1287 nm. However, this set of waveguides support both the fundamental and first-order modes over the considered wavelength range, and the QPM-enhanced mode conversion is found to occur between the higher-order TE_2 mode to TM_1 mode. Therefore it may be assumed that the actual mode conversion efficiency between the TE_2 and TM_1 modes is substantially larger.

QPM nonreciprocal mode conversion has also been demonstrated with single-moded waveguides which have an upper cladding that alternates between Si_3N_4 and a MO film. These were fabricated using a lift-off process that improves the fidelity of the lithographic pattern transfer. With a reduced difference in refractive index in the top cladding media, there should be a commensurate decrease in optical scattering losses.

The CeYFeO MO upper cladding used in these studies was almost certainly neither epitaxial nor in its fully crystalline form (cerium-substituted yttriumirongarnet, CeYIG). Consequently, the Verdet constant of the medium produced, which, from the presence of ferromagnetism is considered to consist of CeYIG crystallites in an amorphous CeYFeO matrix, was expected to be considerably subdued compared to those commonly measured in CeYIG (typically of the order of 3000°/cm). We attempted rapid thermal annealling of these CeYFeO films at temperatures around 750°C where crystallisation to Ce-YIG is expected. However the difference in thermal expansion coefficients between the GaAs substrate and the CeYFeO film resulted in catastrophic fracturing and delamination of the film.

The thermal stress problem can be alleviated by patterning the YIG film to reduce the contact area prior to annealing. Phosphoric acid solutions have successfully wet-etched YIG rib structures on silicon substrates [9], but as it also etches III-V semiconductor it is an unsuitable approach for laser-compatible wafers. Therefore as an alternative we have been developing a PMMA lift-off process for YIG deposition (deposited as amorphous films with partial pressure differential sputtering [10]) in collaboration with University of Minnesota. Initial results are highly promising with a range of YIG sections (typically $\sim$100 μm$\times$1.5 μm) deposited on top of GaAs which remain intact with smooth edges after an anneal in an oxygen atmosphere as shown in fig. 4.

We have demonstrated low-loss reciprocal polarisation mode conversion based on an asymmetric profile rib waveguide using a single wafer etch step. One approach used an angled etch

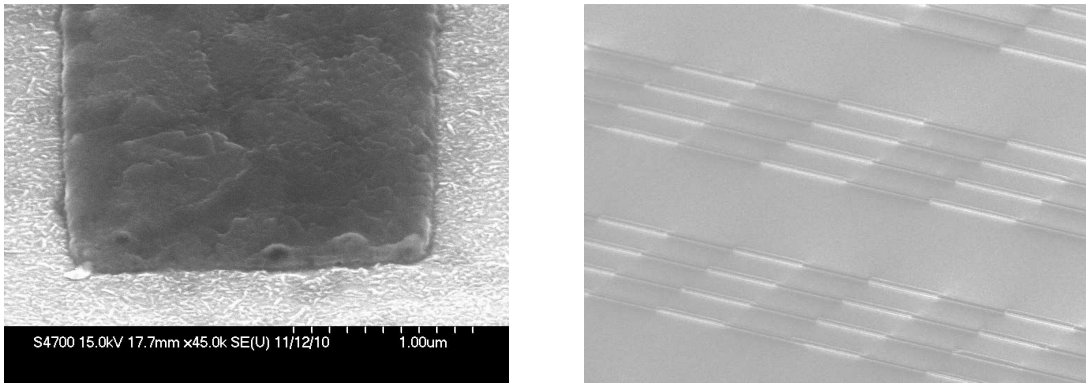

Figure 4: Deposited and annealed YIG sections on GaAs. The left SEM image shows the detail of the edges of the YIG section. The right SEM image shows the upper waveguide cladding after the electron-beam development of an overlayer of SiO_2, which also provides an etch mask for defining a rib waveguide in the semiconductor.

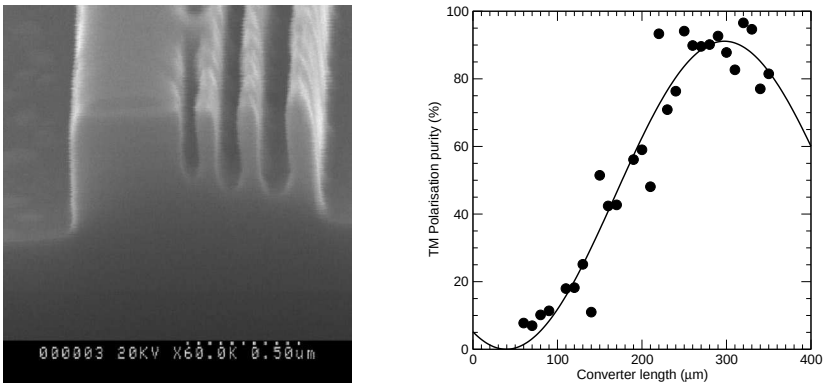

Figure 5: Asymmetric profiled rib waveguide by RIE lag (left). A measurement of TE- to TM-polarisation mode conversion (right).

in a custom sample holder, and was successfully integrated with a semiconductor laser to provide a multiply-polarised output [11]. The second approach utilises the Reactive Ion Etch Lag phenomenon with a normal dry-etching configuration, as shown in fig. 5 [7]. 50% polarisation conversion was achieved with an optical loss of only 0.6 dB. Further refinements were made to the wafer processing steps for the polarisation mode conversion technologies by the incorporation of direct-write hydrogen silsesquioxane (HSQ) hard masks, increasing the fidelity of the waveguide fabrication and reducing further the optical losses.

We have identified that the required integrated device functionalities can be realised with a single specification for the R-PMC: a half-beat length section with an effective optic axis at 22.5° to the wafer surface (or surface normal) such that light injected with solely TE- (or TM-) polarisation produces a 50:50 TE:TM power split at a relative phase of zero (or π). As such the R-PMC provides the role of a 3 dB splitter but between orthogonal polarisation modes rather than a waveguide junction. The R-PMC design constraints are relaxed in comparison to a converter intended to approach 100% TE- to TM-polarisation conversion. Indeed, preliminary simulations indicate a single-trench RIE-lag design with a length of the order of $\sim$100 μm should suffice to meet the

required performance characteristics.

CONCLUSIONS

This paper describes the progress made towards the long-standing goals of integrated nonreciprocal optical devices such as isolators and circulators. Our approach has been to utilise polarisation mode conversion facilitated by Faraday rotation using a longitudinal magnetic field. We have identified three particular issues in the translation of the functionality of bulk components to a waveguide format compatible with semiconductor diode lasers. It has been shown that these can be overcome by incorporating an asymmetric-profile waveguide as a reciprocal polarisation mode converter and by periodic patterning of a magneto-optic/non-magneto-optic upper cladding on a III-V semiconductor rib waveguide to achieve quasi-phase-matched nonreciprocal polarisation mode conversion.

Our initial, proof-of-principle demonstration of QPM nonreciprocal polarisation mode conversion used a low-temperature sputtered CeYFeO film with a relatively modest and inconsistent Verdet coefficient. Such films can be annealed to promote crystallisation to the garnet phase, and with a large Verdet coefficient will facilitate much shorter device lengths. However, the mis-match in thermal expansion between the garnet and the semiconductor does generally lead to a catastrophic failure of the film on annealing at the required temperatures, generally in excess of 700°C. By appropriately limiting the feature size of the garnet prior to annealing, the stresses can be managed to avoid such failures. In collaboration with the University of Minnesota, we have developed a lift-off process for fabricating garnet features suitable for III-V semiconductors. These features are shown to remain intact after annealing in an O_2 atmosphere to promote the garnet crystallisation. Fabrication of rib waveguides incorporating these features is currently underway.

There is some risk that under the annealing temperatures required for the crystallistion of the garnet that the surface of a III-V semiconductor may be compromised, e.g. by Langmuir evaporation resulting in a roughening of the semiconductor surface [12]. Epitaxial MgO buffer layers, as thin as 4.5 nm, grown upon the surface of GaAs have been demonstrated to adequately protect GaAs and preserve the integrity of a quantum well at temperatures in excess of 800°C [13]. It has further been demonstrated that high-quality YIG and CeYIG [14] may be grown upon MgO and hence it is anticipated that the use of a MgO buffer layer may provide protection for the semiconductor surface should it prove necessary.

ACKNOWLEDGMENTS

This work was supported in part by funding from the Engineering and Physical Sciences Research Council (UK). We acknowledge the valuable contributions of Prof. Beth Stadler and Mr. Andy Block, University of Minnesota, for providing the defect-free garnet deposition and annealing facilities used in the development of the garnet lift-off process.

REFERENCES

[1] W. V. Parys, B. Moeyersoon, D. V. Thourhout, R. Baets, M. Vanwolleghem, B. Dagens, J. Decobert, O. L. Gouezigou, D. Make, R. Vanheertum, and L. Lagae, Appl. Phys. Lett. **88**, 071115 (2006).

[2] H. Shimizu, S. Goto, and T. Mori, Appl. Phys. Express **3**, 072201 (2010).

[3] D. C. Hutchings, J. Phys. D **36**, 2222 (2003).

[4] H. Yokoi, T. Mizumoto, and H. Iwasaki, Electronics Letters **38**, 1670 (2002).

[5] P. K. Tien, R. J. Martin, R. Wolfe, R. C. L. Craw, and S. L. Blank, Appl. Phys. Lett. **21**, 394 (1972).

[6] R. Wolfe, J. Hegarty, J. J. F. Dillon, L. C. Luther, G. K. Celler, and L. E. Trimble, IEEE Trans. Magn. **21**, 1647 (1985).

[7] B. M. Holmes and D. C. Hutchings, Photonics Tech. Lett. **18**, 43 (2006).

[8] B. M. Holmes and D. C. Hutchings, Appl. Phys. Lett. **88**, 061116 (2006).

[9] S.-Y. Sung, X. Qi, and B. J. H. Stadler, in *Conference on Lasers and Electro-Optics, Baltimore, MD* (The Optical Society of America, 2007), p. CThN5.

[10] S.-Y. Sung, X. Qi, and B. J. H. Stadler, Appl. Phys. Lett. **87**, 121111 (2005).

[11] J. J. Bregenzer, S. McMaster, M. Sorel, B. M. Holmes, and D. C. Hutchings, J. of Lightwave Tech. **27**, 2732 (2009).

[12] E. J. Tarsa, M. D. Graef, D. R. Clarke, A. C. Gossard, and J. S. Speck, J. Appl. Phys. **73**, 3267 (1993).

[13] B. J. H. Stadler and A. Gopinath, IEEE Trans. Magn. **36**, 3957 (2000).

[14] B. J. H. Stadler, K. Vaccaro, P. Yip, J. Lorenzo, Y. Li, and M. Cherif, IEEE Trans. Magn. **38**, 1564 (2002).